Title
Synchronized network activity in developing rat hippocampus involves regional hyperpolarization-activated cyclic nucleotide-gated (HCN) channel function.

Journal
The European journal of neuroscience, 22(10)

ISSN
0953-816X

Authors
Bender, Roland A
Galindo, Rafael
Mameli, Manuel
et al.

Publication Date
2005-11-01

DOI
10.1111/j.1460-9568.2005.04407.x

Published in final edited form as:
Eur J Neurosci. 2005 November ; 22(10): 2669–2674. doi:10.1111/j.1460-9568.2005.04407.x.

Synchronized network activity in developing rat hippocampus involves regional hyperpolarization-activated cyclic nucleotide-gated (HCN) channel function

Roland A. Bender[1,*], **Rafael Galindo**[2,*], **Manuel Mameli**[2], **Rebeca Gonzalez-Vega**[1], **C. Fernando Valenzuela**[2], and **Tallie Z. Baram**[1]

[1] Departments Pediatrics, Anatomy & Neurobiology, University of California, Irvine, CA 92697–4475, USA

[2] Department of Neurosciences, University of New Mexico, Health Sciences Center, Albuquerque, New Mexico 87131, USA

Abstract

The principal form of synchronized network activity in neonatal hippocampus consists of low frequency 'giant depolarizing potentials' (GDPs). Whereas contribution of both GABA and glutamate to their generation has been demonstrated, full understanding of the mechanisms underlying these synchronized activity bursts remains incomplete. A contribution of the h-current, conducted by HCN channels, to GDPs has been a topic of substantial interest. Here we focus on HCN1, the prevalent HCN channel isoform in neonatal hippocampus, and demonstrate an HCN1 spatiotemporal expression pattern in both CA3 principal cells and interneurons that correlates with the developmental profile of GDPs. Abrogation of HCN physiological function in CA3, via the selective I_h-blocker ZD7288, disrupts GDP generation. Furthermore, ZD7288 specifically abolishes spontaneous bursting of the CA3 pyramidal cells at frequencies typical of GDPs without major influence on interneuronal firing. These findings support a pivotal role for HCN channels expressed by CA3 neurons, and particularly CA3 pyramidal cells, in GDP-related network synchronization.

Keywords

CA3; development; giant depolarizing potentials; interneuron; synchronization

Introduction

Hyperpolarization-activated cyclic nucleotide-gated (HCN) channels, generating I_h, are important determinants of a neuron's excitability (reviewed in Robinson & Siegelbaum, 2003; Santoro & Baram, 2003). They function to maintain resting membrane potential (Lupica *et al*., 2001) and input resistance (Surges *et al*., 2004), and are involved in dendritic summation (Magee, 1998). In addition, HCN channels contribute critically to neuronal network functions, via regulation of rhythmic activity (Pape, 1996; Lüthi & McCormick, 1998) and synchronization of neuronal firing (Maccaferri & McBain, 1996).

Correspondence: Dr Tallie Z. Baram or Dr C. Fernando Valenzuela, as above. tallie@uci.edu or FValenzuela@salud.unm.edu.
*R.A.B. and R.G. contributed equally to this study.

The developing rodent hippocampus expresses three of the four known HCN channel isoforms (HCN1, 2 and 4; Bender *et al*., 2001; Brewster *et al*., 2002, 2005; Vasilyev & Barish, 2002). Expression patterns of individual isoforms change significantly with hippocampal maturation, prompting the consideration that HCN channels may be important for the generation of developmental stage-specific network activity (Bender *et al*., 2001). Focusing on the first postnatal week, our earlier work suggested strong expression of the HCN1 isoform in both pyramidal cells and select interneuronal populations. Hippocampal network activity during this time is unique, consisting primarily of a low-frequency (0.1–0.3 Hz), synchronized activity termed 'giant depolarizing potentials' (GDPs; Ben-Ari *et al*., 1989): i.e. large (25–50 mV), synchronized population discharges, requiring synergistic activation of $GABA_A$ and glutamate receptors (Khazipov *et al*., 1997; Bolea *et al*., 1999).

Contribution of I_h to GDPs has been proposed by Strata *et al*. (1997), who suggested that they are generated by I_h-driven pacemaker cells located in the hilus. Studies demonstrating that CA1 and CA3 neurons can generate GDPs independently of hilar input, and that GDPs originate preferentially in CA3, argued against the proposed pacemaker role of the hilus (Khazipov *et al*., 1997; Menendez de la Prida *et al*., 1998; Bolea *et al*., 1999). However, the contribution of I_h to GDP generation has remained unresolved.

Here we demonstrate that HCN channel function in CA3 is required for GDP generation. Building on earlier work (Bender *et al*., 2001; Agmon & Wells, 2003), we quantify the expression of HCN1 channels in neonatal rat CA3 and hilus. We determine the consequences of pharmacological blockade of HCN channel function on GDP frequency, and record from CA3 minislices to show that I_h in CA3 is sufficient to modulate this activity. Finally, we define a key role for HCN function in CA3 pyramidal cells in the generation of GDPs.

Materials and methods

Immunocytochemistry (ICC)

Experiments were approved by the UCI Animal Care Committee and conformed to NIH guidelines. Immature [postnatal days (P)3, 6 or 10; $n = 3$ each] Sprague-Dawley rats were deeply anaesthetized with sodium pentobarbital (100 mg/kg, i.p.) and transcardially perfused with buffered 4% paraformaldehyde. Brains were cryoprotected, frozen, and cut on a cryostat. Serial sections (40 μm) were first collected from the septal pole of the hippocampus (cut in the coronal plane). Brains were then turned to permit collection of horizontal sections from the temporal pole (see Fig. 1G, inset). HCN1 ICC was performed using polyclonal rabbit anti-HCN1 (1: 2500; Chemicon, Temecula, CA, USA) as described previously (Brewster *et al*., 2002). Cell counts were performed in CA1, CA3 and hilus in five septal and five temporal sections per brain (in both left and right hippocampus; distance between sections: P3, 200 μm; P6, 280 μm; P10, 360 μm). Cell density (neurons per mm^2 of CA1, CA3 or hilar area) was calculated and results were plotted with respect to their septo-temporal position (see Fig. 1G, inset). Data are presented as mean ± SEM. Statistical analysis of septo-temporal variation was performed using one-way ANOVA. For double labelling of HCN1 and glutamic acid decarboxylase (GAD)65, sections were incubated with HCN1 antiserum and monoclonal mouse anti-GAD65 (1: 1500; Chemicon). Antibody binding was visualized with goat anti-rabbit IgG (conjugated to Alexa Fluor 488; 1: 200) and goat-anti-mouse IgG (conjugated to Alexa Fluor 568; 1: 200; Molecular Probes, Eugene, OR, USA) secondary antibodies. To estimate the proportion of interneurons expressing HCN1, colocalization of HCN1 and GAD65 was studied in the most septal and the most temporal section of each series (Fig. 1G, inset). Sections were viewed and photographed with a Nikon Eclipse E400 epifluorescence microscope.

Electrophysiology

Experiments were approved by the UNM-HSC Animal Care Committee and conformed to NIH guidelines. Whole-cell patch-clamp experiments were performed in coronal intact hippocampal slices or CA3 minislices from Sprague-Dawley rat pups (P3–7) as described previously (Carta *et al*., 2003). Animals were anaesthetized with ketamine (250 mg/kg) and 300- to 400-μm coronal slices were prepared on a vibratome. Tissue was incubated and perfused with oxygenated artificial cerebrospinal fluid (ACSF) of the following composition (in mM): NaCl, 126; KCl, 3; NaH_2PO_4, 1.25; $MgSO_4$, 1; $NaHCO_3$, 26; $CaCl_2$, 2; and glucose, 10; equilibrated with 95% O_2 and 5% CO_2. Slices were allowed to recover for 80 min and subsequently perfused with ACSF at a rate of 2–3 mL/min at 32 °C. Recordings were performed under infrared–differential interference contrast microscopy with an Axopatch 200B amplifier (Axon Laboratories, Union City, CA). Microelectrodes had resistances of 3–6 MΩ. GDP currents and $GABA_A$ postsynaptic currents were recorded at a holding potential of −60 mV using the following internal solution (in mM): CsCl, 140; $MgCl_2$, 2; $CaCl_2$, 1; EGTA, 10; HEPES (pH 7.3), 10; Na_2-ATP, 4; and QX-314, 2 (Tocris-Cookson, Ellisville, MO). Current-clamp experiments in CA3 pyramidal cells and interneurons were performed with the following internal solution (in mM): K-gluconate, 115; KCl, 20; disodium phosphocreatine, 10; HEPES (pH 7.3), 10; MgATP, 4; and GTP, 0.3. Spontaneous spikes in CA3 pyramidal neurons and interneurons were recorded with the loose-patch (75–150 MΩ) cell-attached technique in the presence of antagonists of glutamate receptors (100 μM DL-AP5 and 10 μM NBQX) and $GABA_A$ receptors (20 μM bicuculline methiodide). For these studies, electrodes were filled with ACSF. $GABA_A$-mediated currents were pharmacologically isolated by application of glutamate receptor antagonists DL-AP5 (Tocris-Cookson; 100 μM) and NBQX (10 μM). Stratum radiatum interneurons were identified based on their location and morphology using the biocytin labelling method as previously described (Carta *et al*., 2003). Data were acquired with pClamp7 software (Axon Laboratories, Union City, CA, USA) and events were analysed with Minis Analysis program (Synaptosoft, Decatur, GA, USA). Data are presented as mean ± SEM. Drugs ZD7288 and NBQX were prepared in water, DL-AP5 was prepared in 1 N NaOH and tetrodotoxin was prepared in water. All compounds were purchased from Sigma (St Louis, MO, USA) unless otherwise specified.

Results

Distinct developmental gradients of HCN1 channel expression in neonatal hippocampus

Consonant with our findings on HCN1 mRNA expression (Bender *et al*., 2001; Brewster *et al*., 2002, 2005), HCN1 channel protein was already detectable in P3 hippocampus. HCN1 expression in CA3 (Fig. 1A) and CA1 (not shown) pyramidal cells was prominent at this age. In CA3 pyramidal cells, expression declined progressively between P3 and P10, when GDP activity wanes (Fig. 1A, D and G; note that signal in the neuropil in D and G may localize to dendrites, or to basket cell axons; Fig. 1D, inset). HCN1 was undetectable in dentate gyrus granule cells at all ages studied (Fig. 1C, F and I).

In interneuronal populations, HCN1 channels were robustly expressed by numerous cells in CA3 as early as P3 (Fig. 1A and B), when HCN1 expression in interneurons of dentate gyrus (Fig. 1B and C) and CA1 (not shown) was rarely detected. On P3, HCN1-expressing interneurons were found mainly in CA3 strata radiatum and oriens (Fig. 1A). With increasing age, HCN1 expression increased in interneurons associated with the pyramidal cell layer (presumed basket and chandelier cells; Fig. 1D and G). Interestingly, HCN1 was visible in CA3 interneuronal axon terminals as well as in the typical somatic location (Fig. 1D, inset). In addition, whereas the number of HCN1-expressing interneurons in the hilus increased several-fold between P3 and P10 (reflected in a significant increase in cell density;

compare Fig. 1B, E and H), it increased only slightly with maturation in CA3 (~1.5-fold after volume adjustment; Fig. 1B, E and H). Thus, the HCN1 expression pattern in CA3, in both pyramidal cells and interneurons, is supportive of a role of these channels in neuronal activity patterns during the first neonatal days.

A developmental gradient of HCN1 expression in CA3 was also apparent along the septo-temporal hippocampal axis: on P3, significantly more neurons in CA3 strata radiatum and oriens expressed HCN1 channels at the septal compared to the temporal pole (Fig. 1B; one-way ANOVA, $F_{9,20} = 2.9$, $P < 0.05$), and a larger majority of (GAD65-expressing) interneurons at the septal pole co-expressed HCN1 (75 ± 4% vs. 62 ± 2% at the temporal pole). This pattern disappeared with maturation: on P6, 71 ± 2% of septal and 72 ± 3% of temporal interneurons expressed HCN1, and on P10 the corresponding numbers were 62 ± 3 and 66 ± 4%. Note that an analogous developmental gradient was also found in the hilus on P6 (Fig. 1E; one-way ANOVA, $F_{9,20} = 20.5$, $P < 0.001$). Because GDPs preferentially originate at the septal pole (Leinekugel *et al*., 1998), presence of the highest HCN channel expression in this region is concordant with the sites of GDP generation.

Pharmacological blockade of HCN channel function in CA3 reduced GDP frequency and affected pyramidal cell burst firing

The robust expression of HCN channels in both pyramidal cells and interneurons of neonatal CA3 prompted us to examine the functional role of these channels in GDP generation, studying the effects of the selective I_h-blocker ZD7288 on network activity in slices from neonatal (P3–7) hippocampi. In voltage-clamp mode, GDPs were readily recorded in CA3 pyramidal cells of intact hippocampal slices (Fig. 2A, top trace), occurring with frequencies ranging from 0.05 to 0.4 Hz and durations of 0.5–1 s. Application of ZD7288 caused a dose-dependent reduction in GDP frequency (Fig. 2A–C). This effect was quite rapid, excluding nonspecific run-down actions of the blocker (Chevaleyre & Castillo, 2002;Chen, 2004), occurred at low inhibitor doses and persisted after washout of the blocker (Fig. 2A and B). To better localize these effects to HCN channel function in CA3, we repeated these experiments in CA3 minislices. Even in the isolated CA3, application of 40 μM ZD7288 reduced GDP frequency significantly, thus pin-pointing the effect to I_h expressed within CA3 (reduction of GDP frequency: 71 ± 10%; $n = 4$; not shown; compare with Fig. 2C).

I_h is known to play a role in the regulation of neuronal bursting activity (Agmon & Wells, 2003; Cobb *et al*., 2003) and intrinsically bursting pyramidal cells drive GDPs in the immature CA3 region (Sipilä *et al*., 2005). Therefore, we investigated the effect of ZD7288 on CA3 pyramidal cell physiology. Following a hyperpolarizing current injection, four out of four CA3 pyramidal neurons demonstrated the presence of voltage sag and rebound depolarization characteristic of I_h activation (Fig. 3A). Bath application of 1 μM ZD7288 reduced both voltage sag and rebound depolarization (Fig. 3A and B). This effect was detectable as early as 3–4 min after application of the compound, correlating well with the onset of ZD7288 effects on GDP generation. A similar effect was detected with 5 μM ZD7288 ($n = 3$; not shown).

We next obtained loose-patch cell-attached recordings from neonatal CA3 pyramidal cells (Nunemaker *et al*., 2003). In agreement with a recent report (Sipila *et al*., 2005), these neurons burst spontaneously in the presence of blockers of ionotropic glutamate and $GABA_A$ receptors (Fig. 3C). Under control conditions, each burst contained 8 ± 2 spikes and bursts occurred at a frequency similar to that of GDPs: 0.6 ± 0.1 Hz ($n = 4$). In the presence of 1 μM ZD7288, the bursting activity of the CA3 pyramidal neurons was virtually abolished although single action potentials and occasional bursts could still be detected at a frequency of 0.7 ± 0.1 Hz (Fig. 3C and D). Note that the number of spikes/burst and burst frequency as a function of time in the absence of ZD7288 were stable throughout a 15-min

recording period (i.e. 5–6 spikes/burst with a bursting frequency of ≈ 0.5 Hz; $n = 2$; not shown).

In addition to pyramidal cells, four out of five interneurons from CA3 stratum radiatum showed voltage sag and rebound depolarization, which were eliminated by bath application of 40 μM ZD7288 ($n = 3$; not shown). Interestingly, this did not affect the average firing rate of CA3 interneurons (98 ± 4% of control, $n = 7$; Fig. 3E and F) and did not influence the average frequency of $GABA_A$-mediated spontaneous postsynaptic currents arriving at CA3 pyramidal cells (101 ± 1% of control, $n = 6$; Fig. 3E and F). Unlike CA3 pyramidal neurons, CA3 interneurons did not burst spontaneously (Sipilä *et al*., 2005).

Discussion

The principal findings of the present study are as follows. (i) Distribution and developmental gradients of HCN1 channel expression highly support a role of HCN1 within area CA3 in generation and propagation of GDPs. (ii) Pharmacological blockade of HCN channel function in neonatal CA3 profoundly reduces the frequency of GDPs. (iii) HCN channel blockade, at concentrations abolishing GDPs, abrogates bursting activity of CA3 pyramidal cells but does not influence firing frequencies of interneurons. Taken together, these findings suggest that HCN channels in neonatal CA3, and particularly those in pyramidal cells, contribute critically to the generation of GDPs.

GDPs are network-driven events, requiring synergistic activation of hippocampal principal cells and interneurons (Ben-Ari, 2002). The precise contributions of the glutamatergic and GABAergic components of GDP generation have long been a subject of discussion. GABAergic transmission is depolarizing in neonatal hippocampus (attributable to high intracellular Cl^- concentration in immature neurons; Rivera *et al*., 1999), and it has therefore been suggested that the rhythmic firing of the interneuronal network might drive GDPs (Strata *et al*., 1997). In this scenario, it is the interneuronal HCN channels that might contribute critically to GDPs, by generating pacemaker currents (Strata *et al*., 1997) or by contributing to synchronization of principal cell firing (Maccaferri & McBain, 1996).

Alternatively, the major pacing activity resulting in GDPs may originate within pyramidal cells. Indeed, Sipilä *et al*. (2005) have recently provided convincing evidence that neonatal CA3 pyramidal cells show voltage-dependent intrinsic bursting activity that drives the GDPs and is responsible for their preferred frequency of 0.3 Hz *in vitro*, whereas the depolarizing action of GABA is facilitatory without being temporally patterned. Our data are in agreement with the latter hypothesis: intrinsic bursting activity occurred in pyramidal cells but not in interneurons of neonatal CA3. In addition, this pyramidal cell firing required HCN channel function because it was abolished by low concentrations of the I_h blocker ZD7288, which also attenuated GDP generation. In contrast, even much higher concentrations of the blocker had little effect on the firing pattern of interneurons. These data suggest that HCN channel function in pyramidal cells but not in interneurons is essential for GDP generation.

How could HCN channels contribute to the generation and/or propagation of the GDPs? Whereas the explicit role of these channels in pyramidal cells is not fully resolved, several observations in the study by Sipilä *et al*. (2005) provide valuable hints. HCN channels are fundamental to slow depolarization following a firing-evoked after-hyperpolarization. Indeed, the depolarizing ‘sag’ of membrane potential is the typical hallmark of the presence of I_h in a neuron (Pape, 1996; Robinson & Siegelbaum, 2003; Fig. 3A). For the generation of recurrent bursting of CA3 pyramidal cells, which underlie the occurrence of GDPs (Sipilä *et al*., 2005), specific fluctuations of membrane potential are required. These include a postburst afterhyperpolarization followed by slow depolarization to a burst-generating

voltage window. This latter depolarizing current is typical of HCN channel-mediated I_h (Sipilä *et al*., 2005).

In summary, during the first postnatal week, unique expression patterns of HCN1 channels in hippocampal CA3 coincide with a unique developmental activity pattern, the GDPs. Pharmacological blockade of HCN channel function eliminates GDP-promoting bursting activity in CA3 pyramidal cells, even in the isolated CA3. Taken together, these findings support a mechanistic role for HCN channel function within these cells in the generation of GDPs.

Acknowledgments

We wish to thank Dr Yuncai Chen for his excellent contributions and Michele Hinojosa for excellent editorial assistance. This study was supported by NIH Grants NS35439 (T.Z.B.) and AA015614 (C.F.V.).

Abbreviations

DL-AP5	DL-2-amino-5-phosphonovaleric acid
GAD	glutamic acid decarboxylase
GDP	giant depolarizing potential
HCN	hyperpolarization-activated cyclic nucleotide-gated
ICC	immunocytochemistry
I_h	current generated by HCN channels
NBQX	2,3-dioxo-6-nitro-1,2,3,4-tetrahydrobenzo(F)quinoxaline-7-sulfonamide
P	postnatal day

References

Agmon A, Wells JE. The role of the hyperpolarization-activated cationic current I_h in the timing of interictal bursts in the neonatal hippocampus. J Neurosci 2003;23:3658–3668. [PubMed: 12736337]

Ben-Ari Y. Excitatory actions of gaba during development: the nature of the nurture. Nat Rev Neurosci 2002;3:728–739. [PubMed: 12209121]

Ben-Ari Y, Cherubini E, Corradetti R, Gaiarsa JL. Giant synaptic potentials in immature rat CA3 hippocampal neurons. J Physiol (Lond) 1989;416:303–325. [PubMed: 2575165]

Bender RA, Brewster AL, Santoro B, Ludwig A, Hoffmann F, Biel M, Baram TZ. Differential and age-dependent expression of hyperpolarization-activated, cyclic nucleotide-gated channel isoforms 1–4 suggests evolving roles in the developing rat hippocampus. Neuroscience 2001;106:689–698. [PubMed: 11682156]

Bolea S, Avignone E, Berretta N, Sanchez-Andres JV, Cherubini E. Glutamate controls the induction of GABA-mediated giant depolarizing potentials through AMPA receptors in neonatal hippocampal slices. J Neurophysiol 1999;81:2095–2102. [PubMed: 10322051]

Brewster AL, Bender RA, Chen Y, Dube C, Eghbal-Ahmadi M, Baram TZ. Developmental febrile seizures modulate hippocampal gene expression of hyperpolarization-activated channels in an isoform and cell-specific manner. J Neurosci 2002;22:4591–4599. [PubMed: 12040066]

Brewster AL, Bender RA, Yeh A, Shigemoto R, Baram TZ. Quantitative analysis of mRNA and protein expression, and the evolution of sub-cellular transport of the hyperpolarization-activated cyclic nucleotide gated (HCN) channels throughout development in rat hippocampus. Soc Neurosci Abstr 2005;35:377.15.

Carta M, Ariwodola OJ, Weiner JL, Valenzuela CF. Alcohol potently inhibits the kainate receptor-dependent excitatory drive of hippocampal interneurons. Proc Natl Acad Sci USA 2003;100:6813–6818. [PubMed: 12732711]

Chen C. ZD7288 inhibits postsynaptic glutamate receptor-mediated responses at hippocampal perforant path-granule cell synapses. Eur J Neurosci 2004;19:643–649. [PubMed: 14984414]

Chevaleyre V, Castillo PE. Assessing the role of I_h channels in synaptic transmission and mossy fiber LTP. Proc Natl Acad Sci USA 2002;99:9538–9543. [PubMed: 12093909]

Cobb SR, Larkman DM, Bulters DO, Oliver L, Gill CH, Davis CH. Activation of Ih is necessary for patterning of mGluR and mAChR induced network activity in the hippocampal CA3 region. Neuropharmacology 2003;44:293–303. [PubMed: 12604089]

Khazipov R, Leinekugel X, Khalilov I, Gaiarsa JL, Ben-Ari Y. Synchronization of GABAergic interneuronal network in CA3 subfield of neonatal rat hippocampal slices. J Physiol (Lond) 1997;498:763–772. [PubMed: 9051587]

Leinekugel X, Khalilov I, Ben-Ari Y, Khazipov R. Giant depolarizing potentials: the septal pole of the hippocampus paces the activity of the developing intact septohippocampal complex in vitro. J Neurosci 1998;18:6349–6357. [PubMed: 9698326]

Lupica CR, Bell JA, Hofmann AF, Watson PL. Contribution of the hyperpolarization-activated current (I_h) to membrane potential and GABA release in hippocampal interneurons. J Neurophysiol 2001;86:261–268. [PubMed: 11431507]

Lüthi A, McCormick DA. H-currents: properties of a neuronal and network pacemaker. Neuron 1998;21:9–12. [PubMed: 9697847]

Maccaferri G, McBain CJ. The hyperpolarization-activated current (I_h) and its contribution to pacemaker activity in rat CA1 hippocampal stratum oriens-alveus interneurons. J Physiol (Lond) 1996;497:119–130. [PubMed: 8951716]

Magee JC. Dendritic hyperpolarization-activated currents modify the integrative properties of hippocampal CA1 pyramidal neurons. J Neurosci 1998;18:7613–7624. [PubMed: 9742133]

Menendez de la Prida L, Bolea S, Sanchez-Andres JV. Origin of the synchronized network activity in the rabbit developing hippocampus. Eur J Neurosci 1998;10:899–906. [PubMed: 9753157]

Nunemaker CS, DeFazio RA, Moenter SM. A targeted extracellular approach for recording long-term firing patterns of excitable cells: a practical guide. Biol Proced Online 2003;5:53–62. [PubMed: 12734556]

Pape HC. Queer current and pacemaker: the hyperpolarization-activated cation current in neurons. Annu Rev Physiol 1996;58:299–327. [PubMed: 8815797]

Rivera C, Voipio J, Payne JA, Ruusuvuori E, Lahtinen H, Lamsa K, Pirvola U, Saarma M, Kaila K. The K^+/Cl_l^- co-transporter KCC2 renders GABA hyperpolarizing during neuronal maturation. Nature 1999;397:251–255. [PubMed: 9930699]

Robinson RB, Siegelbaum SA. Hyperpolarization-activated cation currents: From molecules to physiological function. Annu Rev Physiol 2003;65:453–480. [PubMed: 12471170]

Santoro B, Baram TZ. The multiple personalities of h-channels. Trends Neurosci 2003;26:550–554. [PubMed: 14522148]

Sipilä ST, Huttu K, Soltesz I, Voipio J, Kaila K. Depolarizing GABA acts on intrinsically bursting pyramidal neurons to drive giant depolarizing potentials in the immature hippocampus. J Neurosci 2005;25:5280–5289. [PubMed: 15930375]

Strata F, Atzori M, Molnar M, Ugolini G, Tempia F, Cherubini E. A pacemaker current in dye-coupled hilar interneurons contributes to the generation of giant GABAergic potentials in developing hippocampus. J Neurosci 1997;17:1435–1446. [PubMed: 9006985]

Surges R, Freiman TM, Feuerstein TJ. Input resistance is voltage dependent due to activation of Ih channels in rat CA1 pyramidal cells. J Neurosci Res 2004;76:475–480. [PubMed: 15114619]

Vasilyev DV, Barish ME. Postnatal development of the hyperpolarization-activated excitatory current I_h in mouse hippocampal pyramidal neurons. J Neurosci 2002;22:8992–9004. [PubMed: 12388606]

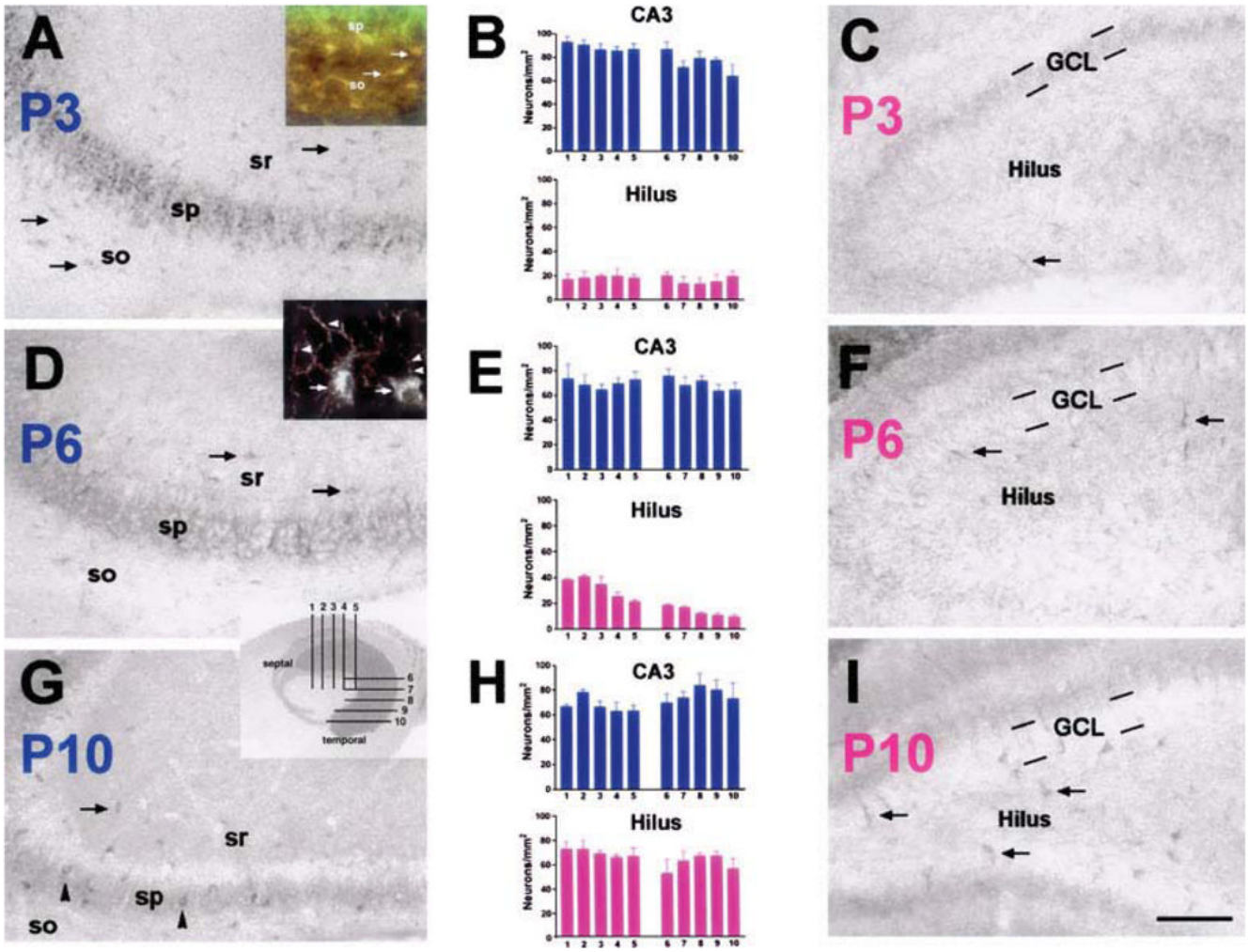

Fig. 1.

Distinct developmental gradients of HCN1 channel expression exist in neonatal hippocampus. HCN1 expression was analysed in (A, D and G) CA3 and (C, F and I) dentate gyrus on (A–C) P3, (D–F) P6 and (G–I) P10. (A) In CA3, HCN1 protein was robustly expressed in pyramidal cells (sp) as early as P3. In addition, a large number of interneurons, mainly located in strata radiatum (sr) and oriens (so), expressed HCN1 in neonatal CA3 (arrows in A). (D and G) With maturation, HCN1 protein expression in pyramidal cells declined. Expression in interneurons remained robust (arrows in D and G) but became more prominent in interneurons of stratum pyramidale (arrowheads in G). (C) In dentate gyrus, few hilar interneurons expressed HCN1 on P3 (arrow). (F and I) Only in the second postnatal week did their number increase substantially (arrows). HCN1 expression was absent in granule cell layer (GCL). Quantitative analyses of HCN1-expressing interneurons (per CA3 or hilar area) on (B) P3, (E) P6 and (H) P10 demonstrated the earlier appearance of the channels in CA3 (blue bars) compared to the hilus (pink bars). These analyses further revealed developmental gradients of HCN1 expression along the longitudinal axis of the hippocampus. Septo-temporal differences were significant in CA3 on P3 (B, blue bars; one-way ANOVA, $F_{9,20} = 2.9$, $P = 0.03$), and in hilus on P6 (E, pink bars; $F_{9,20} = 20.5$, $P < 0.001$; *y*-axis, number of HCN1-positive cells/unit area; *x*-axis, position of sections according to inset in G). Inset in A, double-labelling of HCN1 (green) and GAD65 (red) revealed colocalization in virtually all (≈ 96%) neurons in CA3 stratum oriens on P3

(arrows), demonstrating their GABAergic nature. HCN1-expressing pyramidal cells (sp.) did not express GAD65. Inset in D, high magnification photograph of CA3 on P6, demonstrating HCN1-immunoreactivity in somata of interneurons (arrows) and in (presumably GABAergic) axon terminals innervating CA3 pyramidal cells perisomatically (arrowheads). Scale bar, 100 μm (A, C, D, F, G and I), 50 μ m (inset in A), 20 μ m (inset in D).

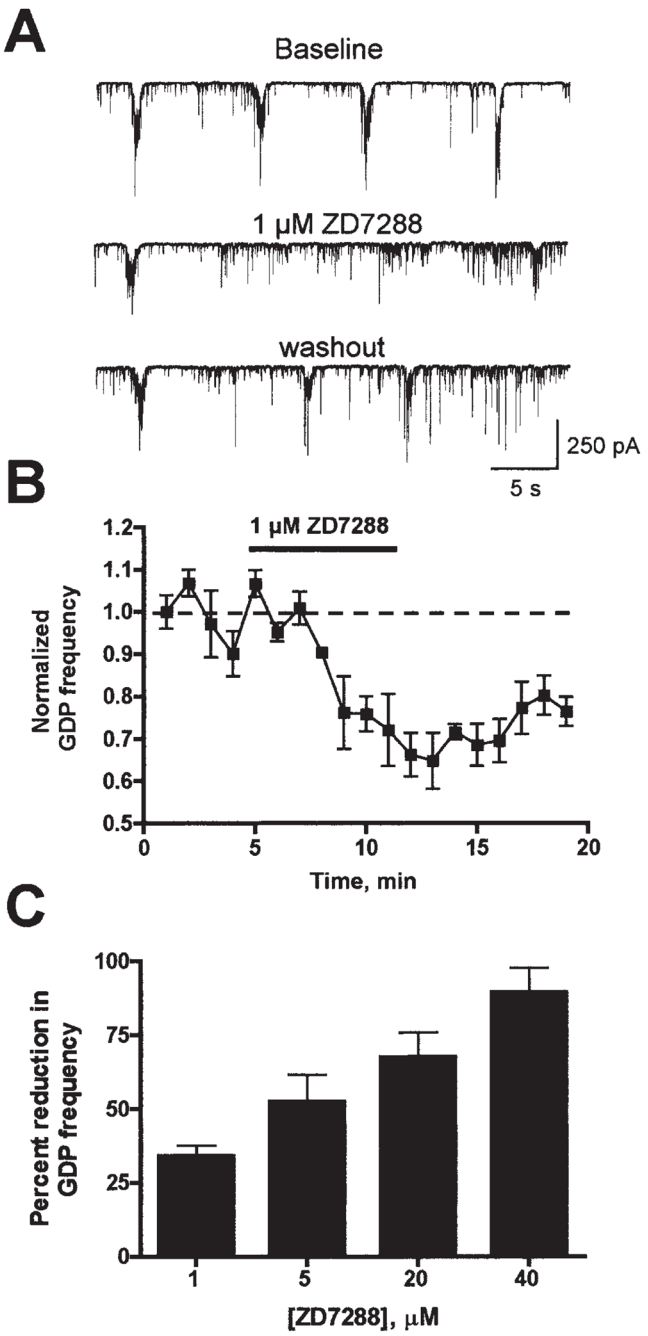

Fig. 2.

Blockade of I_h channel function reduced GDP frequency. (A) Sample traces recorded from a CA3 pyramidal neuron, from a P4 rat, demonstrating the inhibitory effect of 1 μM ZD7288 on GDP frequency. The effect of ZD7288 persisted after washout of the compound (bottom trace). (B) Time course (1-min bin size) of the effect of 1 μM ZD7288 on GDP frequency. (C) Summary of the effect of increasing concentrations of ZD7288 on GDP frequency (n = 3–4).

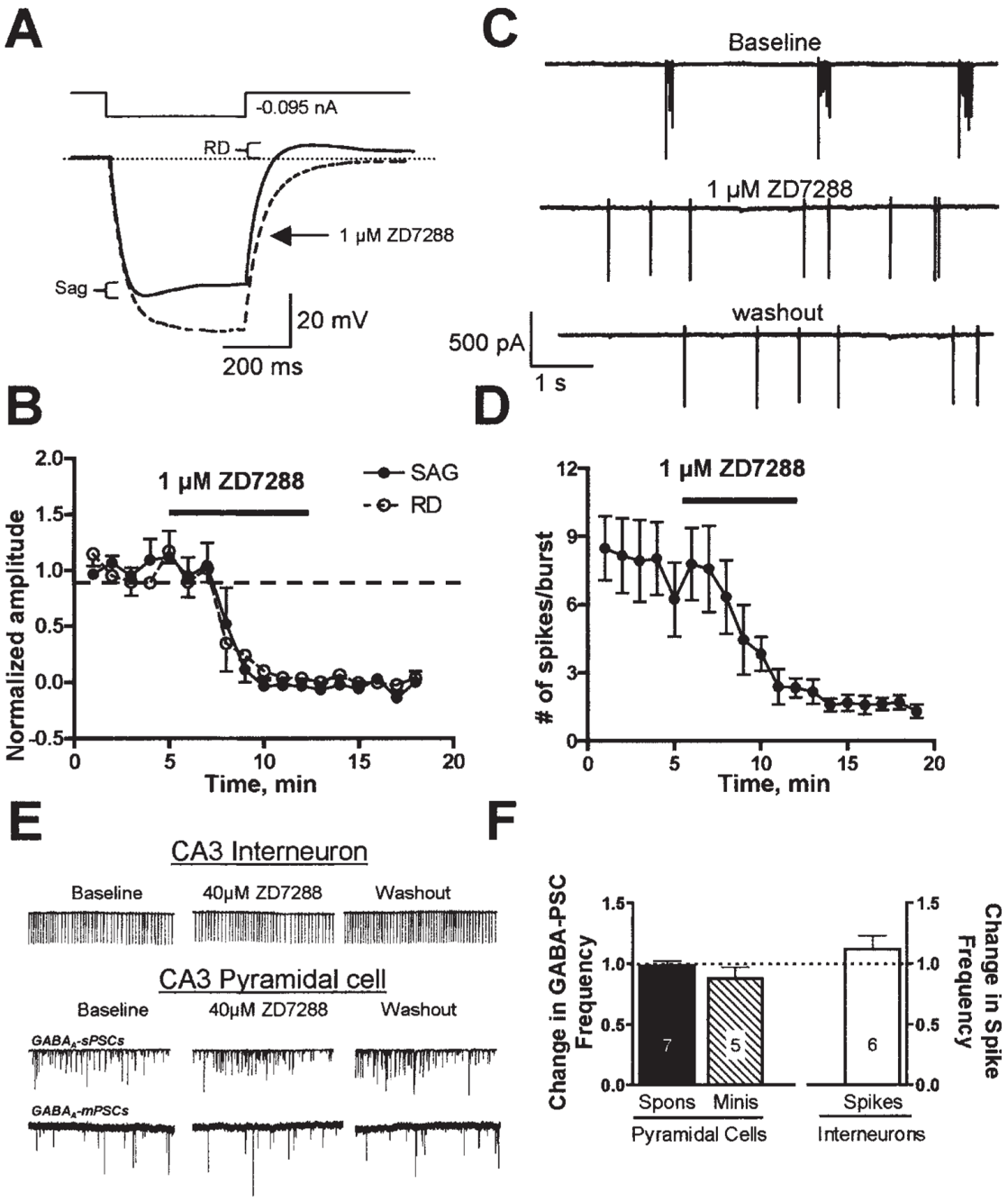

Fig. 3.

Effect of ZD7288 on neonatal CA3 pyramidal cells and interneurons. (A) Pyramidal cells were exposed to a 400-ms hyperpolarizing current step in the absence and presence of 1 μM ZD7288. Note the presence of the hyperpolarizing sag and rebound depolarization (RD) during and after the application of the hyperpolarizing pulse. Both the sag and rebound depolarization were blocked by a 7-min bath application of ZD7288. (B) Time course of the effect of 1 μM ZD7288 on voltage sag and rebound depolarization (n = 4). (C) ZD7288 (1 μM) altered spike bursting firing of CA3 pyramidal cells. (D) Time course of the effect of 1 μM ZD7288 on the number of spikes per burst (n = 4). (E) Even 40 μM ZD7288 did not alter the intrinsic firing frequency of CA3 interneurons, nor did it affect the frequency of

$GABA_A$-mediated spontaneous and miniature postsynaptic currents (PSCs) arriving at CA3 pyramidal cells. (F) Summary of the effects of ZD7288 on average frequency of interneuronal spikes ($n = 6$) and $GABA_A$-mediated synaptic activity (spontaneous, $n = 7$; minis, $n = 5$).